

1 Article

2 

# Photosynthesis of Sago Palm (*Metroxylon sagu* Rottb.)

  
3 

## Seedling at Different Air Temperatures

4 Aidil Azhar<sup>1,†,‡\*</sup>, Daigo Makihara<sup>2,†</sup>, Hitoshi Naito<sup>3,†</sup>, and Hiroshi Ehara<sup>2,4,‡</sup>5 <sup>1</sup> Graduate School of Bioagricultural Sciences, Nagoya University; [aidilazhars@gmail.com](mailto:aidilazhars@gmail.com)6 <sup>2</sup> International Cooperation Center for Agricultural Education, Nagoya University;  
7 [makihara@agr.nagoya-u.ac.jp](mailto:makihara@agr.nagoya-u.ac.jp), [ehara@nuagr1.agr.nagoya-u.ac.jp](mailto:ehara@nuagr1.agr.nagoya-u.ac.jp)8 <sup>3</sup> Collage of Life Science, Kurashiki University of Science and The Arts; [naito@sci.kusa.ac.jp](mailto:naito@sci.kusa.ac.jp)9 <sup>4</sup> Applied Social Science Institute of Asia, Nagoya University; [ehara@nuagr1.agr.nagoya-u.ac.jp](mailto:ehara@nuagr1.agr.nagoya-u.ac.jp)10 \* Correspondence: [aidilazhars@gmail.com](mailto:aidilazhars@gmail.com); Tel.: +81-52-789-4225

11

12 **Abstract:** Photosynthetic activities of the sago palm (*Metroxylon sagu* Rottb.) were studied to find out its sensitivity to changes in ambient air temperature. The minimum ambient air temperature designed for the experiment was 25–29°C, while the higher end was 29–33°C. Several photosynthetic parameters were studied to support our analysis in sago photosynthetic activity, including diurnal leaf gas exchange, assimilation rate vs. CO<sub>2</sub> concentration, leaf greenness, leaf chlorophyll content, and photosynthetic rate vs. irradiance. We found that sago palm photosynthetic activity tends to be more sensitive to minimum than to maximum ambient air temperature. The plants exposed to higher air temperatures had dark green leaf color associated with higher rates of diurnal photosynthesis, chlorophyll content, and rubisco limited photosynthetic activity. They also exhibited higher trend in optimum irradiance absorption level. Consequently, maximum light energy dissipation occurred at higher temperatures.13 **Keywords:** carbon response curve; light response curve; photosynthesis; pigment determination; sago palm14 

### 1. Introduction

15 Ambient air temperature generally has a significant impact the physiological performance of plants. Many studies reveal that inhibition of photosynthetic performance occurs at severely high (&gt;35°C) and low temperatures (&lt;20°C) [1]. However, in the tropical zone in which the sago palm typically grows, variation in air temperature within a year is less than in temperate zones, so this study focused on a moderate air temperature range from 25–33°C to ascertain the sago palm's photosynthetic performance in the ambient air environment of its typical habitat.

16 The sago palm is a perennial monocot crop well known for its potential to accumulate high amounts of starch in its trunk. It can store approximately 300 kg (dry weight) of starch per tree [2]. The importance of sago palm as a staple food is well recognized in some areas of Southeast Asia and South Pacific. The carbohydrate contained in the trunk can be further processed into various basic raw materials for food, animal feed and industrial uses [3]. Coming from the arecaceae or palmae family, sago is able to grow in marginal terrain such as submerged and tidal areas where most agronomy crops cannot survive without drainage or soil improvement. As one of the most important crops for sustainable agriculture and for rural development in swampy areas of Indonesia, sago palm has become an important part of peatland restoration projects.

17 The optimum air temperature range for sago palm is very narrow, reported as from 25°C to 29°C [4]. Elsewhere it has been reported that the best growing conditions required a minimum of at least 26°C [5]. The minimum temperature has been cited as an important factor limiting sago palm performance [6], which is likely due to the tendency of the photosynthesis enzyme Ribulose-1,5-bisphosphate carboxylase/oxygenase (Rubisco) to be very sensitive to air temperature. Minimum temperature reduces rubisco activity, which consequently reduces the utilization of RuBP by rubisco. Rubisco activase content is suppressed by up to 80% at 25°C and below [7]. A study on hibiscus plants reported that the effective quantum yield of PSII ( $\Phi_{PSII}$ ) is suppressed below 10°C [8].18 Regarding maximum temperature, morphological observation of sago palm seedlings reported that at 35°C leaves expanded but become less green [9]. Higher air temperature also plays an important role in sago seed germination. At 30°C, seed germination was about 20% higher than at 25°C [10]. In physiological studies, moderate heat stress affects light energy harvesting as more light is dissipated for non-photochemical quenching rather than photochemical quenching. Therefore, the CO<sub>2</sub> fixation process is depressed [11]. Another study confirmed that carboxylation efficiency decreased at 39°C followed by a reduction in photosynthetic efficiency [12].

19 While it has been considered that variations of ambient air temperature in the sago palm habitat might affect its physiological performance, especially its photosynthetic activity, this has not been definitively proven. This

57 study aimed to provide useful data on sago palm physiology at different air temperatures beyond the little that  
 58 has so far been published. Understanding the regulation of photosynthesis and chlorophyll fluorescence is very  
 59 important as a tool in characterising plant reactions under abiotic stress, such as high and low temperature stress  
 60 [13]. Thereby, the area for sago palm cultivation can be effectively selected to meet the need for appropriate air  
 61 temperature, allowing optimum plant growth to be achieved and producing optimal yields.

62 Due to the abovementioned high degree of photosynthetic sensitivity of the plant, especially at lower  
 63 temperatures, it was hypothesised that even moderate changes in air temperature will inhibit the photosynthetic  
 64 performance of sago palm.

65 **2. Materials and methods**

66 *2.1. Plant material and culture conditions*

67 The experiment was conducted in two phytotrons (glass house) with air temperatures ranging from 25–  
 68 29°C and 29–33°C respectively at Nagoya University, Japan, from January to March 2017. These air  
 69 temperatures were considered as the range of ambient temperature in sago palm habitats associated with tropical  
 70 rainforest climate. Air relative humidity ranged from 30–50% and irradiance flux density from 600–800  $\mu\text{mol}$   
 71  $\text{m}^{-2} \text{s}^{-1}$ . Six one-year-old sago palm seedlings with six fully-developed leaves, grown individually in 1/10000a  
 72 Wagner pots (diameter 115 mm and height 184 mm), were tested. The plant materials were obtained in seed  
 73 form from Sentani District, Jayapura, Indonesia. Vermiculite was applied as the growing media for each plant.  
 74 The nutrients were supplied through the application of Kimura B culture solution. The second youngest leaves  
 75 were selected for all measurements. At the beginning, all plants were placed in the same phytotron with air  
 76 temperature set at 25–29°C. After that six plants were moved to a phytotron with air temperature at 29–33°C.  
 77 After one month of acclimation, measurement was conducted.

78 *2.2. Diurnal leaf gas exchange*

79 Diurnal leaf gas exchange was measured hourly from 7:00 AM to 05:00 PM. The diurnal leaf gas exchange  
 80 measurement was end at 03:00 PM to the plants grown at 25–29°C as the photosynthetic value was zero after  
 81 03:00 PM. The portable photosynthesis system, Li-6400XT (LiCor Inc., USA) with 6  $\text{cm}^2$  leaf chamber was  
 82 utilized during the measurement. The  $\text{CO}_2$  concentration was controlled at 400  $\mu\text{mol}$  and photosynthetic photon  
 83 flux density (PPFD) was set at 750  $\mu\text{mol} \text{ m}^{-2} \text{ s}^{-1}$ . The  $\text{CO}_2$  mixer was adjusted at 500  $\mu\text{mol}$  and relative humidity  
 84 in the leaf chamber was controlled at 40% in the phytotron. During measurement, leaf temperature was set at  
 85 25°C. Net photosynthetic rate ( $P_N$ ), stomatal conductance ( $g_s$ ), transpiration rate ( $T_r$ ), and intercellular  $\text{CO}_2$   
 86 concentration ( $C_i$ ) parameters were obtained from this measurement.

87 *2.3. Assimilation rate vs.  $\text{CO}_2$  concentration (A/Ci curve)*

88 A carbon response curve was constructed following the Farquhar photosynthesis model [14,15] to conceive  
 89 the photosynthesis interference at different air temperatures. Changes in rates of assimilation in response to  
 90 carbon dioxide variation was studied by setting several levels of  $\text{CO}_2$  concentration with constant PPFD  
 91 intensity set at 750  $\mu\text{mol}$ . At the beginning,  $\text{CO}_2$  concentration was set at 400  $\mu\text{mol}$  and gradually reduced to the  
 92 lowest concentration at 50  $\mu\text{mol}$ . After reaching the lowest level,  $\text{CO}_2$  concentration was gradually increased to  
 93 a maximum level of 2000  $\mu\text{mol}$ . Finally,  $\text{CO}_2$  concentration was returned to 400  $\mu\text{mol}$  with irradiance in the “off”  
 94 mode. There were three replicates for each treatment.

95 The A/Ci curves data were obtained by A/Cc curve fitting utility version 1.1 developed by Sharkey [15].  
 96 The derived variables obtained from the fitting curve are maximum carboxylation capacity ( $V_{\text{cmax}}$ ), and electron  
 97 transport rate ( $J$ ) [16]. The Rubisco limited photosynthesis ( $V_{\text{cmax}}$ ) was calculated using the following equation:

$$102 A = V_{\text{cmax}} \left[ \frac{C_c - I^*}{C_c + K_c(1 + O/K_o)} \right] - R_D \quad [1]$$

103  $V_{\text{cmax}}$  represents maximum Rubisco rate in  $\text{CO}_2$  reduction,  $C_c$  is partial  $\text{CO}_2$  pressure at rubisco,  $K_c$  is the  
 104 Michaelis constant of Rubisco for  $\text{CO}_2$ ,  $O$  is the partial pressure of  $\text{O}_2$  at rubisco,  $K_o$  is the inhibition constant of  
 105 Rubisco for  $\text{O}_2$ ,  $I^*$  is the compensation point of photorespiration, and  $R_D$  is dark respiration in which  $\text{CO}_2$  is  
 106 released by the non-photorespiration process.

107 The following equation was used to calculate the RuBP limited photosynthesis:

$$109 A = J \frac{C_c - I^*}{4 C_c + 8 I^*} - R_d \quad [2]$$

110  $J$  represents the RuBP limited photosynthesis for NADPH formation which is utilized in RuBP regeneration  
 111 which takes four electrons per carboxylation and oxygenation [15].

112 *2.4. Photosynthetic rate vs. Irradiance*

113  
 114 A light response curve was constructed using a photosynthesis yield analyzer (MINI-PAM, Walz-Germany)  
 115 after dark adaptation for 20 minutes. Nine irradiance levels were given from zero to 1300  $\mu\text{mol m}^{-2} \text{s}^{-1}$  and each  
 116 irradiance had an interval of 10 seconds to reach to steady state level. Three sago seedlings were choosen as  
 117 replicates. Three leaflets from the second younger leaf of each plant were measured to obtained the mean value  
 118 of each replicate.

119 The fluorescence data including quantum yield photosystem II ( $\Phi_{\text{PSII}}$ ), electron transport rate (ETR), non-  
 120 photochemical quenching (NPQ), and coefficient of non-photochemical quenching (qN), were computed with  
 121 WinControl software (Walz - Germany). The fraction of energy photo-chemically converted in photosystem II is  
 122 represented by  $\Phi_{\text{PSII}}$  which is calculated as:

123

$$124 \Phi_{\text{PSII}} = \frac{F' - F}{F'} = \frac{\Delta F}{F'} \quad [3]$$

125  $F'$  is the maximum fluorescence yield in light adapted sample where all PSII is the open stage.  $F$  is yield  
 126 fluorescence measured briefly before saturation pulse application, and  $\Delta F$  is the increase of fluorescence  
 127 induced by a saturation pulse [17]. The equation used to fit  $\Phi_{\text{PSII}}$  is simple exponential decay function of the  
 128 form  $\Phi_{\text{PSII}} = e^{-x}$  after appropriate scaling,

129

$$\Phi_{\text{PSII}} = \Phi_{\text{PSII max}} \times e^{-k_y \text{PPFD}} \quad [4]$$

130  $\Phi_{\text{PSII}}$  is quantum yield,  $\Phi_{\text{PSII max}}$  is maximum quantum yield at theoretical zero irradiance,  $k_y$  is a scaling constant,  
 131 and PPFD is photon flux density ( $\mu\text{mol (CO}_2\text{)} \text{m}^{-2} \text{s}^{-1}$ ).

132 Electron transport rate (ETR) is calculated by estimating gross photosynthesis using the following equation:

133

$$\text{ETR} = \Phi_{\text{PSII}} \times \text{PPFD} \times 0.5 \times 0.84 \quad [5]$$

134  $\Phi_{\text{PSII}}$  is the effective quantum yield, PPFD is the irradiance, allocation factor (0.5) is the partitioning energy  
 135 between PS II and PS I, and 0.84 is the leaf absorbance factor ( $\alpha_{\text{leaf}}$ ) [18]. Following Ritchie and Bunthawin [19],  
 136 ETR data was fit using non-linear least squares methods calculated as:

137

$$138 \text{ETR} = \frac{\text{ETR}_{\text{max}} \times \text{PPFD}}{\text{PPFD}_{\text{opt}}} \times e^{1-\text{PPFD}/\text{PPFD}_{\text{opt}}} \quad [6]$$

139 The excel routine for fitting Waiting-in-Line curves was utilized to fit the ETR vs. several levels of irradiance  
 140 [20]. The excel routine was obtained personally from Ritchie. The non-photochemical quenching (NPQ)  
 141 parameter corresponds to the loss of potential energy which is dissipated as heat also referred to as  
 142 thermodynamic loss. NPQ is calculated as:

143

$$144 \text{NPQ} = \frac{Y(\text{NPQ})}{Y(\text{NO})} = \frac{F_m - F'}{F'} \quad [7]$$

145 qN is calculated as:

146

$$\text{qN} = \frac{F_m - F'}{F_m - F_0} \quad [8]$$

147  $F$  is yield fluorescence measured briefly before saturation pulse application,  $F_m$  is the maximum fluorescence of  
 148 dark adapted leaf,  $F_0$  is the minimum fluorescence, and  $F'$  is the maximum fluorescence measured at saturation  
 149 pulse. The equation used to fit qN and NPQ vs. irradiance curves is simple exponential saturation functions:

150

$$\text{qN} = \text{qN}_{\text{max}} [1 - \exp(-K_{\text{qN}} \times \text{PPFD})] \quad [9]$$

151 while NPQ was calculated as:

152  $NPQ = NPQ_{max} [1 - \exp(K_{NPQ} \times PPF)]$  [10]  
153

154 PPF is photon flux density,  $K_{qN}$  and  $K_{NPQ}$  are exponential constants,  $qN_{max}$  is the asymptotic maxima for  $qN$ ,  
155 and  $NPQ_{max}$  is the asymptotic maxima for  $NPQ$ .

156  
157 *2.5. Chlorophyll content*  
158

159 A portable chlorophyll meter, SPAD-502Plus (Konica Minolta, Japan) was utilized to measure leaf  
160 greenness of the same leaves chosen for photosynthesis measurement. The same leaves were harvested for  
161 chlorophyll content analysis.

162 Chlorophyll determination was conducted following Arnon [21] and Lichtenthaler [22] after acetone 80%  
163 extraction using a spectrophotometry (UV-1800 Shimadzu). Chlorophyll and carotenoids concentrations were  
164 calculated in  $\mu\text{g gram}^{-1}$  ground sample.

165  
166 *2.6. Statistical analysis*  
167

168 This experiment employed completely randomized design with two ranges of air temperature, 25–29°C  
169 and 29–33°C, with three replicates. The second upper- most leaf from each replicate was used for measurement.  
170 Each datum is presented as mean  $\pm$  SE. Statistical differences were tested by student *t*-test.

171  
172 **3. Results**  
173

174 *3.1. Diurnal leaf gas exchange*

175 Data for sago palm data show considerable differences in net photosynthetic rate ( $P_N$ ), stomatal  
176 conductance ( $g_s$ ), and leaf transpiration rate ( $T_r$ ) values between the two air temperature ranges (Fig. 1A). The  
177 open circles represent the  $P_N$  of sago palm seedlings growing at 25–29°C room temperature while the closed  
178 circles represent the  $P_N$  of seedlings grown at 29–33°C room temperature. In the first daily measurement at 7:00  
179 h sago seedlings growing at the higher room temperature started with a higher  $P_N$  than the seedlings growing at  
180 lower temperature. The plants grown at 25–29°C maintained the optimum  $P_N$  for a short period as the down-  
181 ward trend began around 12:00 h.

182 Stomatal conductance ( $g_s$ ) and leaf transpiration rate ( $T_r$ ) showed the same trend with  $P_N$ . At 25–29°C,  $g_s$   
183 showed a slight upward trend during the observation. Low stomatal aperture at 25–29°C caused a reduction in  $T_r$   
184 (Fig. 1B,D). At 29–33°C, the higher  $P_N$  trend was followed by higher  $g_s$  and  $T_r$ . However, intercellular  $\text{CO}_2$   
185 concentration ( $C_i$ ) at higher temperature showed a lower rate only in the first two hours of measurement (7:00 to  
186 8:00 h) and the last two hours of measurement. They exhibited almost the same trend in  $C_i$  rate between 9:00  
187 and 13:00 h (Figure 1C).

188  
189 *3.2. Photosynthetic activity and chlorophyll content*  
190

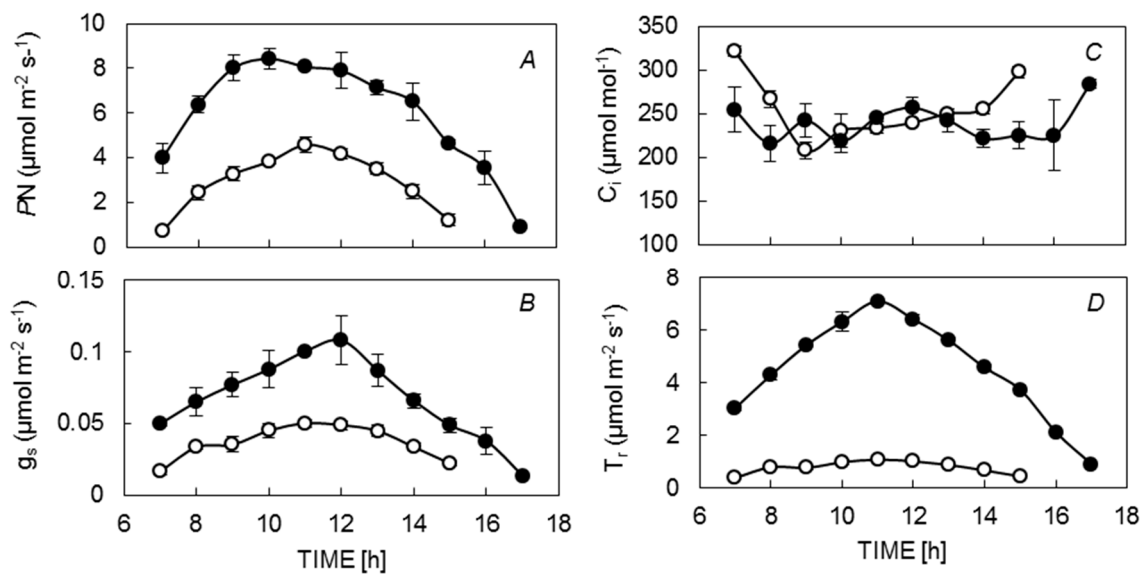
191 Photosynthetic activity and chlorophyll content of sago palm seedlings showed lower rates and  
192 concentrations respectively at 25–29°C air temperature. The low  $P_N$  value was followed by lower values in  
193 biochemical limiting photosynthetic activities such as electron transport rate ( $J$ ) and maximum carboxylation  
194 capacity ( $V_{cmax}$ ). The other parameters to explained the low  $P_N$  at minimum air temperature was pigmentation.  
195 Chlorophyll content seems to be lower at minimum than at higher air temperatures tested. Although only Chl *b*  
196 showed significant difference in pigment content, all parameters were considerably higher in sago seedlings  
197 grown at 29–33°C air temperature (Table 1).

198

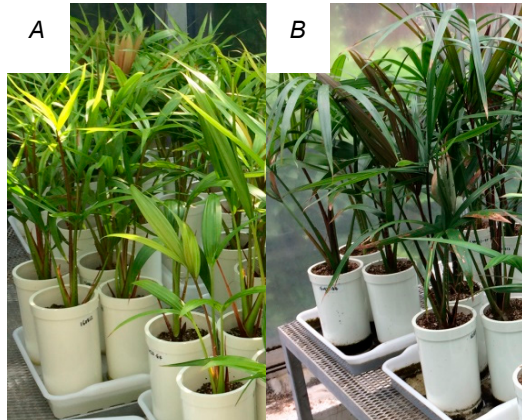
199 **Table 1.** Photosynthetic parameters, and chlorophyll content of sago palm seedlings at different air temperatures.  
200 \*: significant ( $p \leq 0.05$ ), \*\*: significant ( $p \leq 0.01$ ), ns: not significant ( $p > 0.05$ ), respectively using Student *t*-test.  
201 Means  $\pm$  SE,  $n = 3$ .  
202

Parameters	25–29°C	29–33°C
$P_N$ [ $\mu\text{mol (CO}_2\text{ m}^{-2} \text{s}^{-1}$ ]	$5.66 \pm 0.91$	$8.62 \pm 0.24^*$
$J$ [ $\mu\text{mol m}^{-2} \text{s}^{-1}$ ]	$88.2 \pm 10.98$	$114.1 \pm 5.59^{\text{ns}}$
$V_{\text{cmax}}$ [ $\mu\text{mol m}^{-2} \text{s}^{-1}$ ]	$40.1 \pm 10.23$	$99.3 \pm 10.86^*$
SPAD	$46.2 \pm 1.56$	$62.3 \pm 1.91^{**}$
Chl <i>a</i> [ $\mu\text{g g}^{-1}$ ]	$838.1 \pm 34.39$	$987.3 \pm 99.04^{\text{ns}}$
Chl <i>b</i> [ $\mu\text{g g}^{-1}$ ]	$258.5 \pm 10.56$	$319.2 \pm 11.45^*$
Chl <i>a+b</i> [ $\mu\text{g g}^{-1}$ ]	$1096.6 \pm 35.9$	$1306.5 \pm 102.8^{\text{ns}}$
Carotenoid [ $\mu\text{g g}^{-1}$ ]	$223.7 \pm 2.91$	$255.0 \pm 2.91^{\text{ns}}$

203



204 **Figure 1.** Diurnal change in [A] net photosynthetic rate ( $P_N$ ), [B] stomatal conductance ( $g_s$ ), [C] intercellular  
205  $\text{CO}_2$  concentration, [D] transpiration rate ( $T_r$ ) of sago palm seedlings growing at different room temperatures. ○:  
206 25–29°C, ●: 29–33°C. (Mean  $\pm$  SE,  $n = 3$ ).  
207  
208  
209  
210  
211  
212  
213  
214  
215  
216  
217  
218

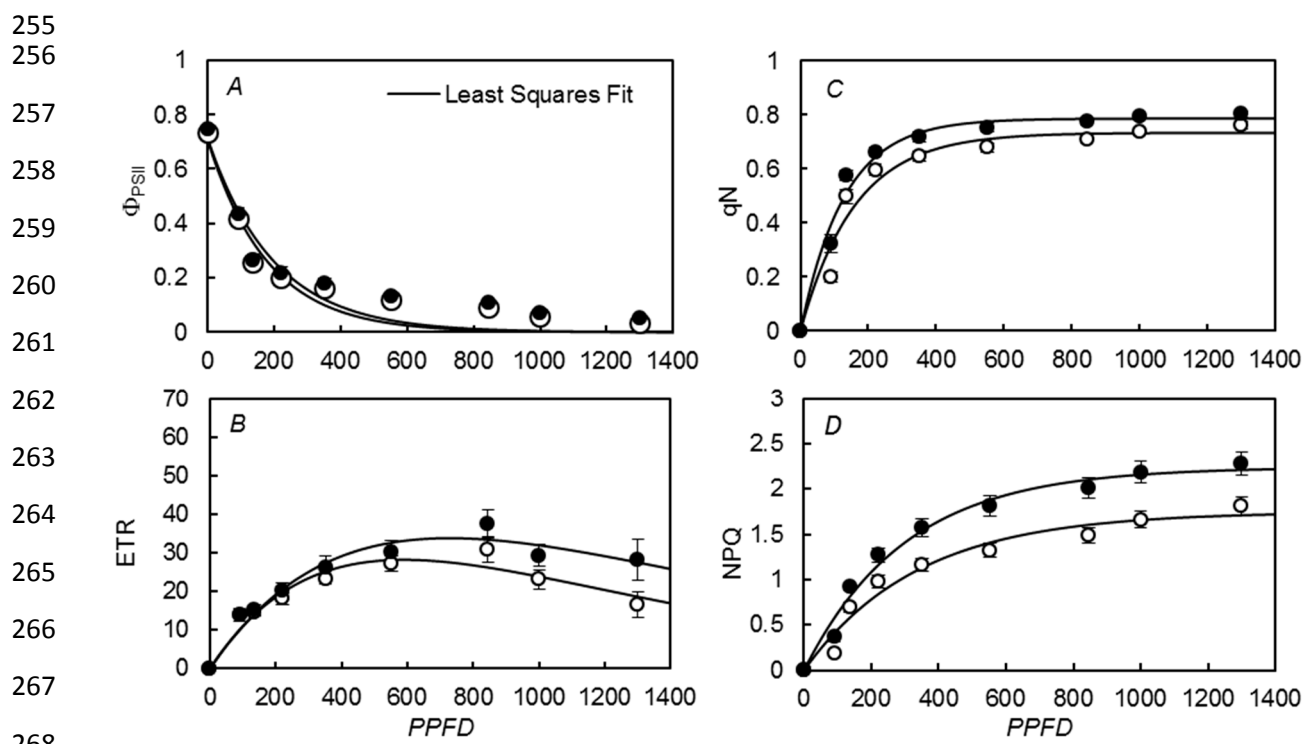


219 **Figure 2.** The leaf greenness of sago palm seedlings grown at 25–29°C [A], and 29–33°C [B] room temperature.  
220  
221  
222  
223  
224  
225  
226  
227  
228  
229  
230  
231  
232  
233  
234  
235  
236  
237  
238  
239

240 The leave color of sago palm grown at 29–33°C was obviously darker than at the lower air temperature  
 241 tested and was confirmed by significantly higher SPAD values. In addition, we noticed that most plants showed  
 242 leaf emergence at the higher air temperature, although no measurement in leaf emergence rate undertaken.  
 243

244 *3.3. Photosynthetic rate vs. Irradiances*

245 Photosynthetic rate vs. Irradiances was measured and fit using non-linear least square fit. The graphics of  
 246 quantum yield of PSII at both air temperatures were obtained (Fig. 3A). The curve of quantum yield of PSII  
 247 ( $\Phi_{PSII}$ ) vs. irradiance at both air temperatures provided a maximum effective quantum yield ( $\Phi_{PSII\ max}$ ) value at  
 248 25–29°C and 29–33°C. The Waiting-in-Line equation was used to fit ETR values (Fig. 3B) for both air  
 249 temperature ranges tested. The variables obtained PPFD<sub>opt</sub>, ETR<sub>max</sub> and  $\alpha_o$  are shown in Table 2. The fitted qN  
 250 and NPQ data (Fig 3C,D) provide information about qN<sub>max</sub> and NPQ<sub>max</sub>. Most of variables in Table 2 are  
 251 dominated by the sago seedlings growing at 29–33°C air temperature. However, according to statistical analysis,  
 252 there are no significant differences in maximum efficiency quantum yield ( $\Phi_{PSII\ max}$ ), maximum electron  
 253 transport rate (ETR<sub>max</sub>), asymptotic photosynthetic efficiency ( $\alpha_o$ ), and maximum coefficient of non-  
 254 photochemical quenching (qN<sub>max</sub>) between the two air temperature ranges.



269 **Figure 3.** (A) Photosynthetic yield ( $\Phi_{PSII}$ ), (B) electron transport rate (ETR), (C) coefficient non-photochemical  
 270 quenching (qN), and (D) non-photochemical quenching (NPQ) vs. irradiance of sago palm seedlings (estimated  
 271 via non-linear least square fitting) at 25–29°C (○) and 29–33°C (●). Mean  $\pm$  SE,  $n = 3$ , with 9 irradiance levels.

272  
 273 **Table 2.** Photosynthetic parameters (fitted by Waiting-in-Line equation) of sago palm seedling at 25–29°C and  
 274 29–33°C air temperatures (Means  $\pm$  SE,  $n = 3$  plants, 27 data points). \*: significant ( $p \leq 0.05$ ), ns: not significance  
 275 ( $P > 0.05$ ) as the results of Student *t*-test.

Parameters	25–29°C	29–33°C
Maximum yield ( $\Phi_{PSII\ max}$ )	$0.70 \pm 0.013$	$0.70 \pm 0.025$ ns
Optimum PPFD (PPFD <sub>opt</sub> )	$587.00 \pm 29.81$	$725.59 \pm 33.32$ *
Maximum electron transport rate (ETR <sub>max</sub> )	$28.28 \pm 2.53$	$33.91 \pm 3.76$ ns
Asymptotic Photosynthetic efficiency ( $\alpha_o$ )	$0.13 \pm 0.006$	$0.13 \pm 0.009$ ns
qN <sub>max</sub>	$0.73 \pm 0.015$	$0.79 \pm 0.014$ ns
NPQ <sub>max</sub>	$1.75 \pm 0.08$	$2.25 \pm 0.13$ *

277 **4. Discussion**

278 At the beginning of measurement (7:00 h) sago palm seedlings revealed low photosynthetic rates in both  
279 treatments. This might be due to the light not reaching sufficient levels for optimum stomatal aperture as blue  
280 light induces the aperture of stomata [23]. Moreover, air temperature at that time has not reached the optimum  
281 level for higher rubisco activity. Consequently, with an increase in light intensity and air temperature from  
282 8:00–11:00 h,  $P_N$ ,  $g_s$ , and  $T_r$  trended upwards in both treatments. However, the plants showed midday depression  
283 as photosynthetic rate reduced from 12:00. This might be caused by stomatal and other non-stomatal limitations  
284 such as photoinhibition, photorespiration and reduction of rubisco activity under high temperature [24]. This is  
285 consistent with most field work cases, where it is difficult to obtain optimum  $P_N$  rate in sago palm when the  
286 measurement is conducted after 12:00 h. This information was confirmed by our findings from diurnal leaf gas  
287 exchange data. In addition, our data suggests that lower air temperature inhibited the seedlings' capacity to  
288 maintain a longer  $P_N$  rate. Higher temperatures (29–33°C) appear to induce higher rubisco activity in sago palm  
289 seedlings than that achieved at lower temperatures (25–29°C) (Table 1). Although producing the same diurnal  
290 leaf gas exchange trend across both air temperature ranges, the sago seedlings growing at 29–33°C room  
291 temperature showed higher photosynthetic rate.

292 According to the data from figure 1A, a lower net photosynthetic rate at 25–29°C was followed by lower  
293 stomatal conductance results in lower leaf transpiration rate. Low transpiration rate is considered to be one of  
294 the factors causing low  $P_N$  rate as CO<sub>2</sub> can only enter leaves through gas diffusion [23]. However, the  
295 intercellular CO<sub>2</sub> concentration (C<sub>i</sub>) did not show higher rate at 25–29°C. C<sub>i</sub> revealed almost the same trend in  
296 both air temperature ranges, except in the first two hours of measurement and the last two hours of measurement  
297 (Fig. 1C). When plants performed higher assimilation rates, intercellular CO<sub>2</sub> value should show a lower rate as  
298 the CO<sub>2</sub> is utilized during photosynthesis activity. Therefore, we assume that at 25–29°C, the photosynthetic  
299 activity was not only limited by those components but also the other components such as rubisco activity, leaf  
300 chlorophyll content and the light harvesting system.

301 In the lower air temperature range (25–29°C), the performances of rubisco activity ( $V_{cmax}$ ) tend to be low.  
302 Low rubisco activity at 25°C might be due to the reduction in RuBP regeneration [25,7]. RuBP regeneration  
303 might be affected by the lower RuBP consumption by rubisco. This could suggest that the activation state of  
304 rubisco could be different in plants grown at different air temperatures.

305 The higher performance in net photosynthetic rate of sago palm seedlings at higher temperatures tested  
306 also could not be separated from the support of higher photosynthetic apparatus formation, such as leaf  
307 chlorophyll. The higher temperatures induced higher formation of leaf pigments such as Chl *a*, Chl *b* and  
308 carotenoid. The sago seedlings grown at higher air temperatures produced leaves with a dark green color, while  
309 sago seedlings grown at lower air temperature produced light green leaves. An appropriate air temperature  
310 increases the capacity for thermotolerance which increases chlorophyll a:b ratio [26,27]. Air temperature also  
311 influences the formation of chlorophyll as temperature regulates the synthesis of chlorophyll precursor [28]. In  
312 our study, the phytotron at 29–33°C provided an appropriate growth environment for sago palm seedlings. Those  
313 growing at 31°C revealed higher uptake in macronutrients such as N, P, K, and Ca, which contribute to the  
314 maximum leaf area [9]. Therefore, it appears the higher uptake of nutrients induced the higher formation of leaf  
315 chlorophyll leading to greater capacity to harvest light energy. In addition, although no measurement in leaf  
316 emergence rate undertaken, we noticed that most plants showed leaf emergence at the higher air temperature,  
317 the same occurrence had previously been found in the study of sago palm seedlings' response to various ranges  
318 of air temperature. It was found that at 35°C leaf emergence rate increased although shoot elongation rate, leaf  
319 area and root growth rate decreased. However, at 23°C leaf emergence rate decreased along with increased root  
320 growth rate [9].

321 In general, sago palm reach light saturation point from 600–750  $\mu\text{mol m}^{-2} \text{s}^{-1}$  PPFD, although this point  
322 may vary depending on the leaf age and shaded conditions [29,6]. According to our finding, air temperature is  
323 also one of the factors affecting the light saturation point of sago palm seedlings, especially in the lower air  
324 temperature range tested. The optimum irradiances (PPFD<sub>opt</sub>) of sago palm seedlings was rather low at 25–29°C  
325 followed by early reduction in electron transport rate as photo inhibition might have occurred due to excess light  
326 energy. This can be seen from the down-ward trend which occurred when the light intensity increased above  
327 600  $\mu\text{mol}$  (Figure 3B). The sago palm seedlings grown at 29–33°C maintained higher performance in light  
328 energy utilization for electron transport than those at 25–29°C (Figure 2B). The increase in leaf temperature as  
329 long as it does not exceed the upper thermal limit, may enhance photon flux density which consequently affects  
330 the adjustment of thermotolerance in PSII and results in optimum photosynthetic rate [30,31,27]. In our study,  
331 sago palm photosynthetic optimum irradiance was higher when the plants were growing at the higher air  
332 temperature. The reduction in electron transport rate due to photo inhibition occurred when PPFD increased  
333 above 800  $\mu\text{mol}$  (Fig. 3B). However, the higher maximum electron transport rate showed not significant higher  
334 between the treatment.

335        Although the sago seedlings grown at higher temperature performed higher optimum irradiance, the  
336        utilization of light energy for photosynthetic activity tends to be less efficient. High dissipation of light energy  
337        in non-photochemical quenching (NPQ) at 29–33°C also supports this analysis. The process is a plant  
338        mechanism to protect the photosynthetic apparatus from photo damage due to excess light energy [32]. Non-  
339        photochemical quenching dissipates the excess of light energy as heat.

340        **5. Conclusion**

341        According to the above findings, we conclude that sago palm photosynthetic performance is affected by  
342        changes in ambient air temperature especially at the minimum air temperature tested. This refers to the lower  $P_N$   
343        performance at air temperatures ranging from 25–29°C as compared to those at 29–33°C. Low  $P_N$  was brought  
344        about by low values in other supporting variables such as stomatal conductance, leaf transpiration rate,  
345        maximum rubisco rate in  $\text{CO}_2$  reduction, and optimum irradiance. A low level of formation of photosynthetic  
346        pigment also becomes a limiting factor in photosynthetic rate at the lower temperatures tested. Consequently,  
347        the harvesting and utilization of light energy for photosynthetic activities was affected. From this it could be  
348        concluded that the optimum air temperature would be associated with higher sago palm yield. Further  
349        investigation of photosynthetic response to different air temperatures using fully grown sago palms is needed to  
350        ascertain whether they show the same photosynthetic performance as in the seedling stage. If such study is able  
351        to confirm the broader representativeness of the present study, the findings might be used to make important  
352        decisions regarding the location of sago palm cultivation areas in the future for optimal production.

353        **Acknowledgement**

354        This article's publication is due in large part to support from The Indonesia Endowment Fund for  
355        Education under the auspices of the Ministry of Finance of the Republic of Indonesia as the sponsor for the main  
356        author's doctoral research scholarship.

357

358        **References**

- 359        1. Larcher, W. *Physiological plant ecology*. Springer. **2003**, pp. 504.
- 360        2. Ehara, H. 2005. Geographical distribution and specification of *Metroxylon* palms. *Jap. J. Trop. Agr.* **2005**,  
361        *49*, 111–116.
- 362        3. Ehara, H.; Susanto, S.; Mizota, C.; Shohei, H.; Tadashi, M. Sago palm (*Metroxylon sagu*, Areaceae)  
363        production in the eastern archipelago of Indonesia: Variation in morphological characteristics and pith-dry  
364        matter yield. *Econ. Bot.* **2000**, *54*, 197–206.
- 365        4. Flach, M.; Braber, K.D.; and Frederix, M.J.J. Temperature and relative humidity requirement of young  
366        sago palm seedlings. pp.139–143. In *Proc. The Third Int. Sago Sym*; Yamada, N.; and Kainuma, K. Eds.  
367        May 20–23. The Sago Palm Research Fund. Tokyo, Japan, **1986**.
- 368        5. Schuiling, D.L. Growth and development of true sago palm (*Metroxylon sagu* Rottboll) with special  
369        reference to accumulation of starch in the trunk, a study on morphology, genetic variation and ecophysiology  
370        and their implications for cultivation. PhD Thesis Wageningen University, Netherlands, **2009**, pp. 3–9.
- 371        6. Okazaki, M.; and Kimura, S.D. Ecology of the sago palm. In: K. Smith, editor, *The sago palm; the food*  
372        and environmental challenges of the 21<sup>st</sup> century, Kyoto Univ. Press. Japan. **2015**, pp. 41–60.
- 373        7. Yamori, W.; Caemmerer, S.V. Effect of rubisco activase deficiency on the temperature response of  $\text{CO}_2$   
374        assimilation rate and rubisco activation state: insights from transgenic tobacco with reduced amount of  
375        rubisco activase. *Plant Physiol.* **2009**, *151*, 2072–2082.
- 376        8. Paredes, M.; and Quiles, M.J. The effect of cold stress on photosynthesis in hibiscus plant. PLOS ONE,  
377        **2015**, doi:10.1371.
- 378        9. Irawan, A.F.; Yamamoto, Y.; Miyazaki, A.; and Tetsushi, Y. Effect of various ranges of controlled air  
379        temperatures on the early growth of sago palm (*Metroxylon sagu* Rottb.) seedlings. *Trop. Agr. Develop.*  
380        **2011**, *55*, 68–74.
- 381        10. Ehara, H., C. Komada, and O. Morita. Germination characteristics of sago palm seeds and spine emergence  
382        in seedlings produced from spineless palm seeds. *Principes*, **1998**, *42*, 212–217.
- 383        11. Mathur, S.; Agrawal, D.; and Jajoo, A. Photosynthesis: response to high temperature stress. *J. Photoch.*  
384        *Photobio. B.* **2014**, *137*, 116–126.
- 385        12. Hew, C.S.; Krotkov, G.; and David, T. Effects of temperature on photosynthesis and  $\text{CO}_2$  evolution in light  
386        and darkness by green leaves. *Plant Physiol.* **1968**, *44*, 671–677.
- 387        13. Maxwell, K.; and Johnson, G.N. Chlorophyll fluorescence – a practical guide. *J. Exp. Bot.* **2000**, *345*,  
388        659–668.
- 389        14. Farquhar, G.D.; Caemmerer, V.S.; Berry, J.A. A biochemical model of photosynthetic  $\text{CO}_2$  assimilation in  
390        leaves of C3 species. *Planta*, **1980**, *149*, 78–90.

- 391 15. Sharkey, T.D.; Bernacchi, C.J.; Farquhar, G.D.; Singsaas, E.L. Fitting photosynthetic carbon response  
392 curves for C3 leaves. *Plant Cell and Environ.* **2007**, *30*, 1035–1040.
- 393 16. Sharkey, T.D. What gas exchange data can tell us about photosynthesis. *Plant Cell Environ.* **2016**, *39*,  
394 1161–1163.
- 395 17. Klughammer, C.; and Schreiber, U. Complementary PSII quantum yields calculated from simple  
396 fluorescence parameters measured by pam fluorometry and the saturation pulse method. PAM Application  
397 Notes, **2008**, *1*, 27–35.
- 398 18. Björkman, O.; and Demmig, B. Photon yield of O<sub>2</sub> evolution and chlorophyll fluorescence characteristics  
399 at 77 K among vascular plants of diverse origins. *Planta*. **1987**, *170*, 489–504.
- 400 19. Ritchie R.J.; and Bunthawin, S. The use of pulse amplitude modulation (PAM) fluorometry to measure  
401 photosynthesis in a CAM orchid, *dendrobium* SPP. (D. CV. Viravuth pink). *Int. J. Plant Sci.* **2010**, *171*,  
402 575–585.
- 403 20. Apichatmeta, K.; Sudsiri, C.J.; Ritchie, R.J. Photosynthesis of oil palm (*Elaeis guineensis*). *Sci. Hortic.*  
404 *Amsterdam*. **2017**, *214*, 34–40.
- 405 21. Arnon, D. I. 1949. Copper enzymes in isolated chloroplasts: Polyphenoloxidase in *Beta vulgaris*. *Plant*  
406 *Physiol.* **1949**, *24*, 1–15.
- 407 22. Lichtenthaler, H. K. Chlorophylls and carotenoids: Pigments of photosynthetic membranes. *Meth. Enzym.*  
408 **1987**, *148*, 350–382.
- 409 23. Taiz, L.; and Zeiger, E. 2012. Plant physiology, fifth ed. Sinauer Associates Inc., Publishers, Sunderland,  
410 Massachusetts, U.S.A, **2012**; pp. 106–130.
- 411 24. Koyama, K.; and Takemoto, S. Morning reduction of photosynthetic capacity before midday depression.  
412 *Sci. Rep.* **2014**, doi: 10.1038.srep04389.
- 413 25. Cen, Y.P.; and Sage, R.F. The regulation of ribulose-1,5-bisphosphate carboxylase activity in response to  
414 variation in temperature and atmospheric CO<sub>2</sub> partial pressure in sweet potato. *Plant Physiol.* **2005**, *139*,  
415 1–12.
- 416 26. Camejo, D.; Rodríguez, P.; Morales, M.A.; Dell'Amico, J.M.; Torrecillas, A.; Alarcón, J.J. High  
417 temperature effects on photosynthetic activity of two tomato cultivars with different heat susceptibility. *J.*  
418 *Plant Physiol.* **2005**, *162*, 281–289.
- 419 27. Wahid, A.; Gelani, S.; Ashraf, M.; Foolad, M.R. Heat tolerance in plants: An Overview. *Environ. Exp. Bot.*  
420 **2007**, *6*, 199–223.
- 421 28. Beck, W.A., R. Redman. Seasonal variation in the production of plant pigments. *Plant Physiol.* **1940**, *15*,  
422 81–94.
- 423 29. Uchida, N., S. Kobayashi, T. Yasuda, and T. Yamaguchi. Photosynthetic characteristics of sago palm,  
424 *Metroxylon rumphii* Martius. *Jpn. J. Trop. Agr.* **1990**, *34*, 176–180.
- 425 30. Salvucci, M.E., and S.J. Crafts-Brandner. 2004. Inhibition of photosynthesis by heat stress: the activation  
426 state of rubisco as a limiting factor in photosynthesis. *Physiol. Plant.* **120**:179–186.
- 427 31. Marchand, F.L.; Mertens, S.; Kockelbergh, F.; Louis, B; and N. Ivan, N. Performance of high arctic tundra  
428 plants improved during but deteriorated after exposure to a simulated extreme temperature event. *Global*  
429 *Change Biol.* **2005**, *11*, 2078–2089.
- 430 32. Ruban, A.V.; and Horton, P. Spectroscopy of non-photochemical and photochemical quenching of  
431 chlorophyll fluorescence in leaves; evidence for a role of the light harvesting complex of photosystem II in  
432 the regulation of energy dissipation. *Photosynth. Res.* **1994**, *40*, 181–190.
- 433
- 434
- 435
- 436
- 437
- 438